

Experimental simulations of pollen coronas

Werner B. Schneider and Michael Vollmer

A procedure to experimentally simulate pollen coronas is discussed. Observed coronas are due to pine and birch pollen having different geometries. Using computer simulations, two-dimensional projections of a large number of pollenlike objects with adjustable shapes, with or without preferential orientation and statistical or regular spatial distribution, are generated. The photograph of the printout allows samples with typical sizes between 20 and 200 μm . Their diffraction patterns can closely resemble the ones observed in nature and predicted by theory. © 2005 Optical Society of America

OCIS codes: 010.1290, 010.1310.

1. Introduction

Coronas are fascinating optical phenomena that usually may be observed as a sequence of colored rings around Sun or Moon, if thin clouds are between them and the observer.^{1–6} Most explanations are based on Fraunhofer diffraction theory for the far field with spherical cloud droplets as obstacles.¹ In addition, color theories explain the perceived hues.

With the availability of modern computers, the limits of applicability of the simple diffraction theory have been explored by comparison of its results with those from the complete Mie theory.^{7–9} As a result the explanation of coronas as due to Fraunhofer diffraction works quite well for spherical particles with typical sizes above 10 μm . Meanwhile, Mie-theory computations can be done with standard PCs, and freeware programs are available to theoretically simulate coronas from water droplets in full color.^{10,11} Theoretical predictions are in good agreement with quantitative analysis of natural observations as well as with laboratory experiments.

Coronas due to cloud droplets usually have spherical symmetry. However, occasionally, droplet size variations or phase changes within a cloud may lead to “broken” symmetrical coronas.¹²

Some years ago, two kinds of asymmetric naturally

occurring coronas were observed¹³ that were neither due to water droplet nor to ice crystals, but rather to pollen floating in the air. The first type has ellipsoidal symmetry, whereas the second one shows additional brightening at top, bottom, and the sides.¹³ Since then, many observations of these “elliptical coronas” have been reported (Fig. 1). They are attributed to diffraction by oriented pollen grains for different kinds of trees like birch or pine.^{13,14} The pollen grains are released by trees in very short periods, depending on weather conditions, thus resulting in concentrations that are sufficient for visual observations. The individual grains have irregular shapes, which would lead to diffraction patterns of spherical symmetry if distributed statistically. However, if they float in the air with preferred orientation, similar to the case of hexagonal ice crystals, as responsible for parhelia, the diffraction patterns are asymmetric. Figure 2 shows an example of the shapes of typical pollen spores of birch, pine, and spruce, respectively.

Theoretically, diffraction patterns of many different shapes have been investigated like, e.g., triangles, trapezoids, and hexagons,¹⁵ hexagonal cylinders, and spheroids.¹⁶ A major theoretical problem with nonspherical shapes is that Mie theory applies to spheres, and it can only be extended to spheroids. Therefore, many theoretical approaches approximated Mie theory by Fraunhofer diffraction, i.e., diffraction patterns were usually calculated from numerical simulations for Fraunhofer diffraction, whenever more complex geometries are present, such as for the pine pollen.¹⁴ Sometimes nonspherical elongated shapes were approximated by spheroids, such as for the birch pollen.¹³

Early experiments studied diffraction patterns from single apertures of various geometries such as disks, portions of disks, and many other irregular

W. B. Schneider (werner.schneider@physik.uni-erlangen.de) is with Physikalisches Institut, Didaktik der Physik, University of Erlangen, Staudtstrasse 7, Erlangen 91058, Germany. M. Vollmer (vollmer@fh-brandenburg.de) is with the University of Applied Sciences Brandenburg, Magdeburger Strasse 50, Brandenburg 14770, Germany.

Received 18 January 2005; revised manuscript received 19 May 2005; accepted 19 May 2005.

0003-6935/05/275746-08\$15.00/0

© 2005 Optical Society of America



(a)



(b)

Fig. 1. Examples of two naturally occurring elliptical coronas (courtesy Jari Piikki) of the first and second kind owing to pollen (see also Ref. 13).

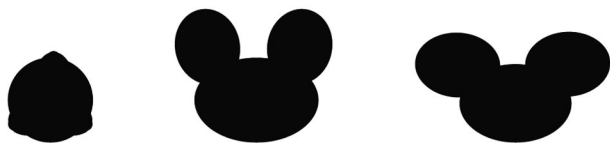


Fig. 2. Example of the shapes of pollen spore of birch (left), pine (middle), and spruce (right) after Ref. 13.

shapes.^{1,17,18} Pollen experiments usually use Lycopodium spores, which are nearly spherical. They are well suited for lecture demonstrations^{1,3,19} but have also been used for quantitative measurements of the diffraction pattern from single Lycopodium spores and spore dimers.²⁰

Whereas coronas experiments with small spheres or circular disk-shaped obstacles are easy to set up, also with respect to tests of theory,^{1,6} no such experiments have been reported so far, to our knowledge, on pollen coronas. This is probably because only a few pollen (e.g., Lycopodium) are easily available commercially, and the geometrical irregularities are usually avoided in simple diffraction experiments. The Lycopodium powder is not suited to study asymmetric pollen coronas, since the spores are nearly spherical in shape such that even single spores produce patterns of nearly spherical symmetry.²⁰

Such experiments could, however, serve two purposes. First, they may be used as experimental demonstrations for diffraction from a sample of a large number of irregularly shaped objects, and second, they could help to quantitatively test diffraction theories of such particles. For complicated shapes, only numerical simulations of the diffraction patterns are possible, and it would be desirable to have an easy means to very quickly visualize the diffraction pattern for given geometries.

The present paper describes how to simulate pollen samples of adjustable geometries and size and to study the diffraction patterns of a large number of these pollen, either statistically distributed or with preferential orientation.

2. Method

Quantitative diffraction experiments usually simplify the setup by first replacing the three-dimensional objects by their two-dimensional projection as opaque disks. For spherical droplets this *flat mask* diffraction is a reasonable approximation for sizes above $10\ \mu\text{m}$, i.e., the Fraunhofer diffraction pattern of the two-dimensional disk then corresponds quite nicely to the Mie-scattering pattern concerning shape and position of the maxima for the three-dimensional droplet.²¹ Since pollen are usually larger than $10\ \mu\text{m}$ (the samples described below will have larger diameters) the samples will also use two-dimensional projections of the three-dimensional shapes.

The second simplification that is often encountered in experiments consists in replacing the sample with disklike opaque objects on a transparent screen by the inverse sample with disklike apertures in an opaque screen. This is motivated by Babinet's principle, which states, that, with exception of the exact forward direction, both diffraction patterns look the same. To make it even more simple, many demonstration experiments of coronas begin with the diffraction pattern of just a single aperture in an opaque screen. In contrast, we describe the preparation of samples of many two-dimensional pollen projections as opaque scatterers.

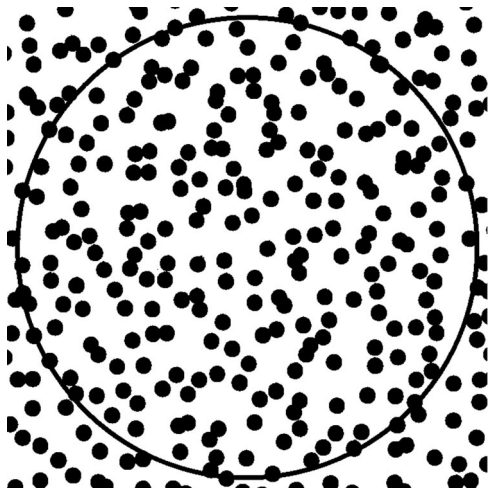


Fig. 3. Example of statistically distributed circular disks of about $100\ \mu\text{m}$ radius on a slide.

A. Generating the Samples

The sample preparation consists of two steps. First, a computer program is used to generate a two-dimensional array of objects. Second, the printout of this program is scaled down photographically such that mean sizes are in the 20 to $200\ \mu\text{m}$ range on the sample slide.

The computer program used to generate samples²² allows the following geometries: circular disks (which give regular coronas), circular rings (for simulation of glories), and various noncircular geometries to approximate known pollen shapes.^{13,23,24} The randomness of the spatial distribution of the disks can be varied between 100% (perfect randomness) and 0% (regular arrangement on a rectangular array). In addition, nearest-neighbor distances may be varied, and the noncircular pollen-shapelike scatterers have the additional option of introducing a preferential orientation.

By taking pictures of the printout of the program from a sheet of paper (size about $20\ \text{cm}$ by $30\ \text{cm}$), the size of the scatterers used in this work was reduced by a factor of about 15 to 20 such that the disks on the slide finally had diameters of the order of 100 to $200\ \mu\text{m}$. It is important that the printer has good resolution; in this work, $600\ \text{dpi}$ was used. For lower-resolution printers, it is recommended to print larger

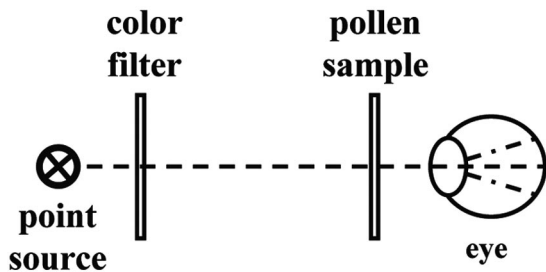


Fig. 4. Experimental setup for observing white-light or colored light diffraction patterns from samples. The sample is placed directly in front of the eye, and a distant light source is observed.

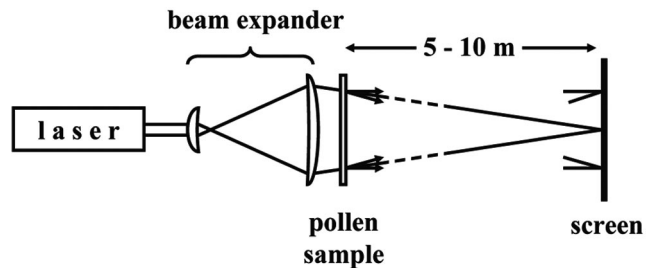


Fig. 5. Experimental setup for projecting monochromatic coronas on a screen.

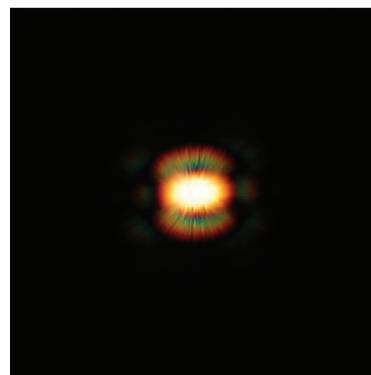
scattering objects and later reduce the size further photographically. As an example, Fig. 3 shows part of the slide with circular disks as samples while indicating the size of an illuminating expanded laser beam by the circle. The laser usually covers of the order of several hundred disks, i.e., the respective diffraction pattern will be due to many disks.

B. Experimental Setup of Diffraction Experiments

Experiments with different light sources and observation conditions are possible. Two setup schemes are used: one for white-light observations, and another one for studying diffraction patterns with monochromatic light.



(a)



(b)

Fig. 6. White-light corona of pollen-shaped scatterers (pine pollen) with (a) random orientation and (b) preferential orientation. In both cases, the scatterers were spatially distributed randomly.

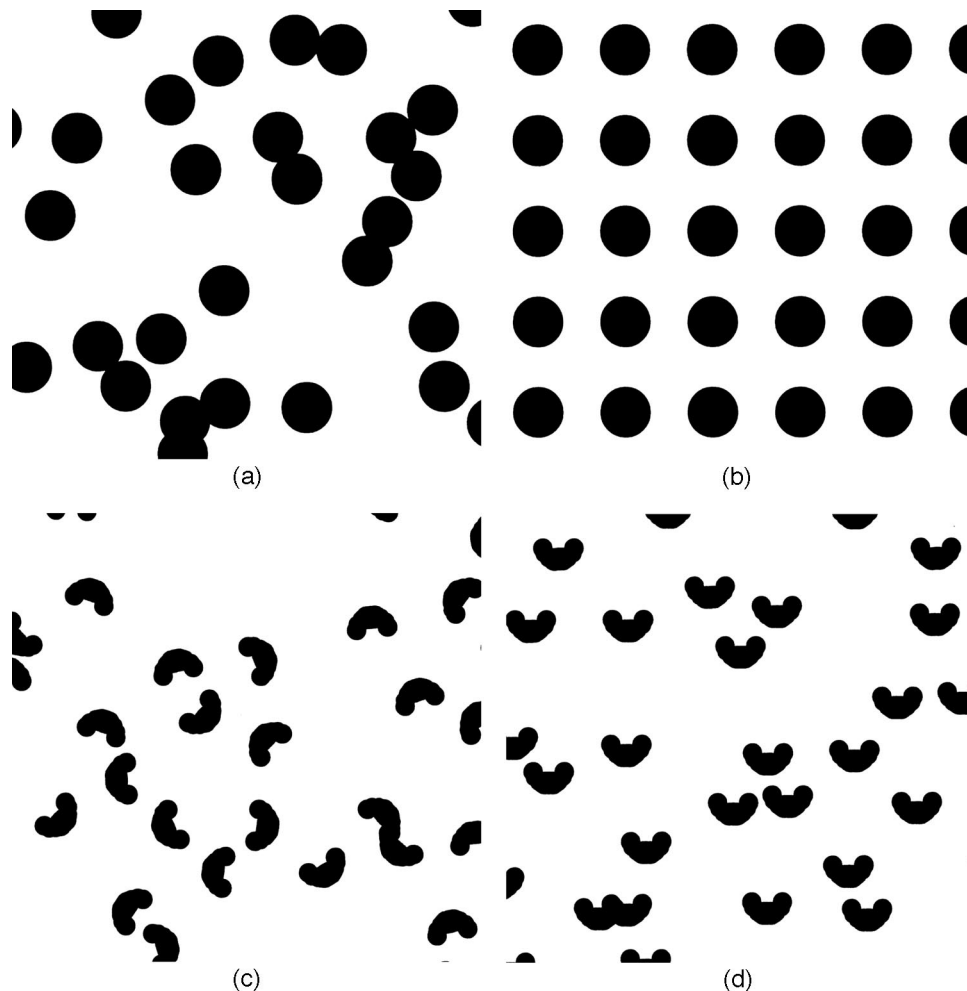


Fig. 7. Slide with four different samples. Circular disks, (a) randomly distributed and (b) in a regular array; pollen-shaped scatterers of random spatial distribution with (c) randomly distributed orientations and (d) with preferential orientation.

White-light sources do not usually have enough intensity for projecting colored diffraction patterns, as observed in nature, onto a white screen. Therefore, the experimental setup shown in Fig. 4 is used for observations with white light. The slide with the pollen sample is placed close to the eye (or camera). The slide is then illuminated by a distant point source of white light such as a 20 W halogen lamp in a distance of several meters or a LED white-light torch without the lens and reflecting mirror. (This setup also allows nearly monochromatic corona structures to be studied by inserting a color filter. Alternatively, a laser beam can be directed onto a screen or sheet of paper, giving rise to a nearly pointlike source of monochromatic light.)

The second setup, shown in Fig. 5, is used for monochromatic light from lasers such as red He-Ne lasers and laser diodes or green frequency-doubled Nd:YAG lasers. The latter two are also available as laser pointers.

With typical laser beam diameters of only 1–2 mm, the nonexpanded beam only illuminates a small number of disks. Therefore the total intensity, which is due to adding the intensities of each illuminated

disk, is very small. Hence the signal-to-noise ratio is low compared to using an expanded laser beam, and it is much harder to resolve the structures of the outer rings with very low light intensities. Therefore, in the following experiments the laser is expanded using a two-lens design (see Fig. 5) before it illuminates the sample.

If the laser beam would be perfectly parallel behind the second lens, the Fraunhofer diffraction pattern behind the slide would be in infinity. Practically, several meter distances are sufficient. There are two alternative methods to observe the diffraction pattern on the screen. Either another lens is placed behind the sample and the screen is fixed in a distance of its focal length, or the position of the second lens of the beam expander is adjustable. The beam expander is then used as a slightly misaligned Keplerian telescope, i.e., the diffraction pattern is projected as an image on the distant screen. Since the second lens of the beam expander is very close to the sample, the beam behind it is nearly parallel, i.e., the diffraction pattern is not changed due to the slight nonparallel illumination. For photos a transparent screen was used, and the camera was placed behind it. In order

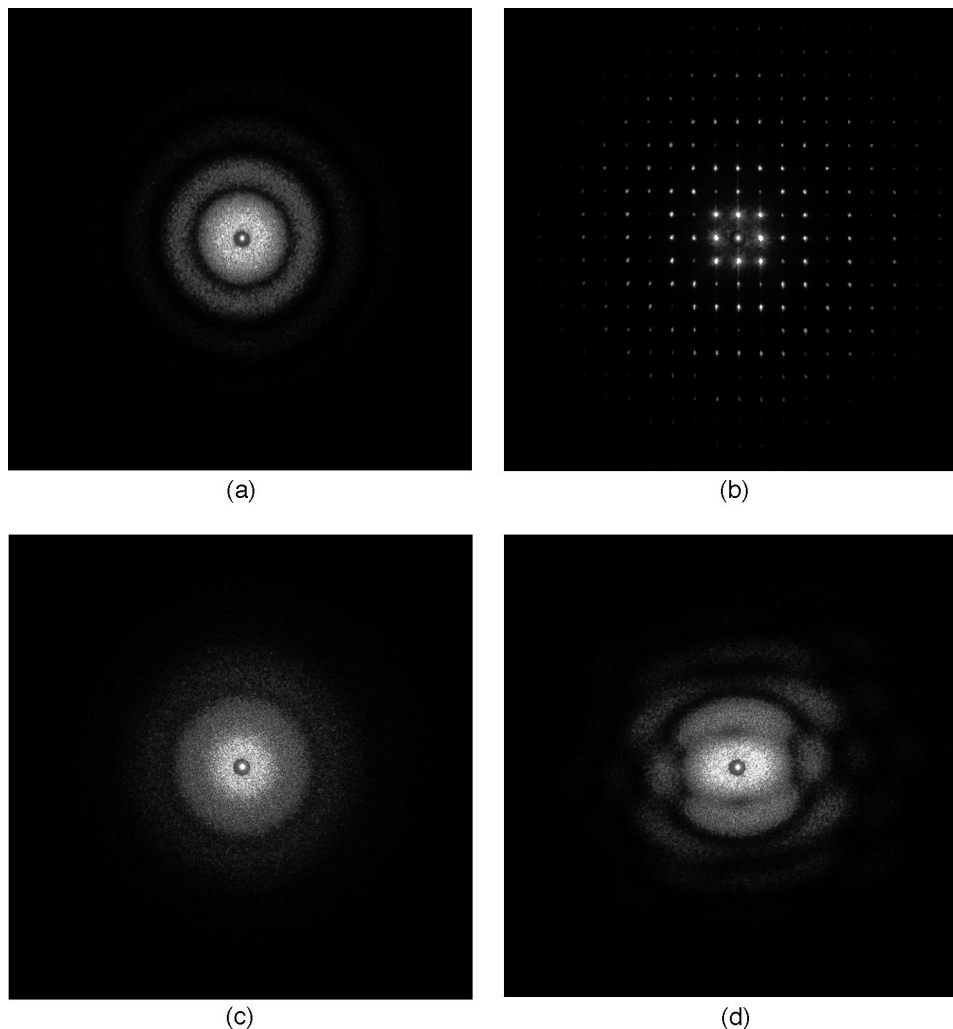


Fig. 8. Diffraction patterns of red light ($\lambda = 632.8 \text{ nm}$) for objects of Fig. 7. Circular disks with (a) random spatial distribution and (b) distribution on a periodic square lattice; pollen-shaped disks of random spatial distribution with (c) random orientation and (d) preferential orientation. The central spot has been attenuated in order to avoid overexposure.

to avoid overexposure of the film, the intensity of the central laser spot on the screen was attenuated by attaching a small circular disk of paper on the screen. This results in small artificial dark rings within the central aureole of all monochromatic diffraction patterns shown below.

3. Results and Discussion

A. Coronas with White Light

Using the setup of Fig. 4, observers immediately see a colored corona diffraction pattern. Figure 6 gives an example of statistically distributed versus oriented pollen disks of about $200 \mu\text{m}$ diameter with random spatial distribution. Here the eye was replaced by the camera. Obviously there are marked differences between the two cases. The pollen with random orientation more or less resemble the corona from spherical water droplets or near spherical pollen spores such as Lycopodium, while other pollen such as spruce or pine are usually oriented. The preferential orientation leads to totally different diffraction patterns.

We note that the absolute size of the disks (relative to the wavelength of the light) affects the angular size of the diffraction pattern but not the geometry of the diffraction pattern, which is governed by the shape of the individual disks. Provided the angular resolution is large enough to separate the fringes, it is more favorable to use larger disk sizes, since they lead to a smaller angular region of the diffraction pattern. In this case, the light intensities from individual fringes are larger compared to the ones from smaller disks whose pattern has a larger angular spread. This is particularly important for outer-lying structures. Therefore we chose diameters of about $100 \mu\text{m}$ to $200 \mu\text{m}$, i.e., larger than is known from natural pollen with sizes between $20 \mu\text{m}$ and $100 \mu\text{m}$. In order to better understand the dependencies on geometry, experiments with monochromatic light of lasers were performed.

B. Diffraction Patterns from Monochromatic Light

Figure 7 depicts a sample slide, which contains four different samples. Linear dimensions of the individ-

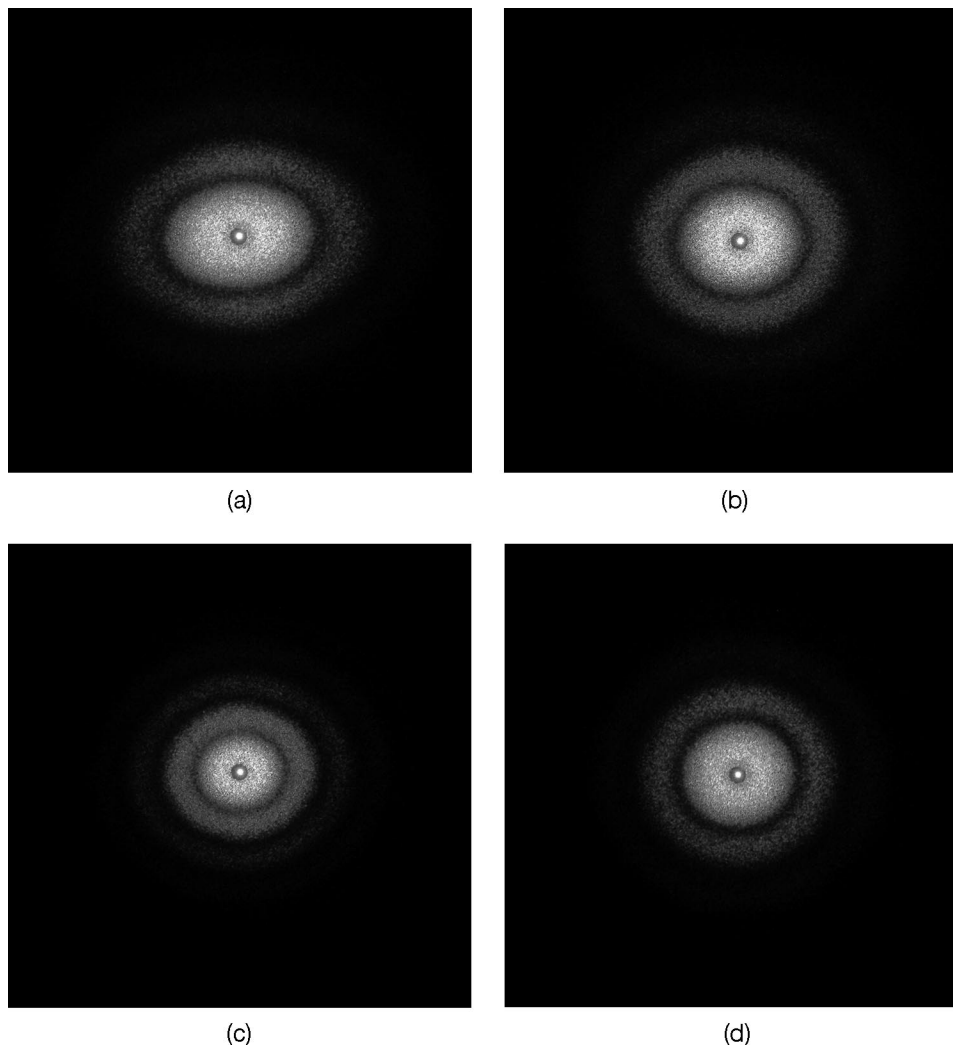


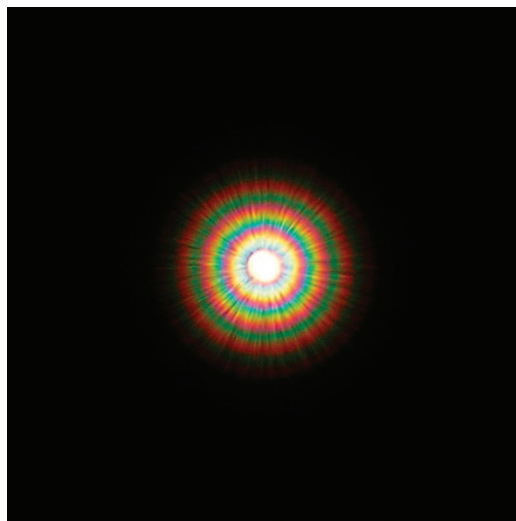
Fig. 9. Diffraction pattern of red light ($\lambda = 632.8$ nm) for a random distribution of preferentially oriented ellipsoids with different aspect ratios (a) 0.6, (b) 0.8, (c) 0.85, and (d) 0.9. The central spot has been attenuated in order to avoid overexposure.

ual scatterers on the slide are about $200 \mu\text{m}$. On top, the diffraction objects are circular disks with a spatial arrangement being either random or regular; on bottom, pollen-shaped disks as in Fig. 6 are depicted. They are randomly distributed; however, they may have preferred orientation or randomly distributed orientations. Their geometry represents pine pollen.

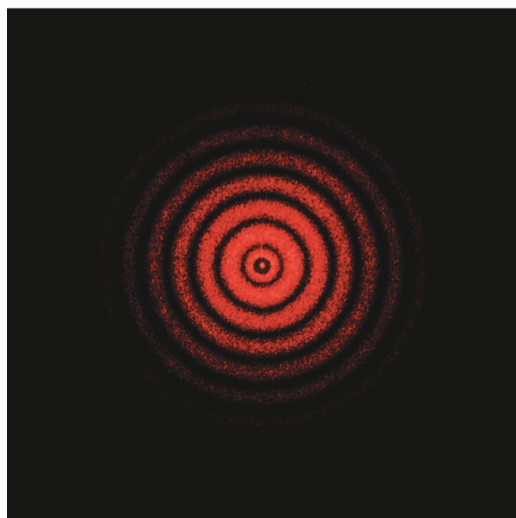
Figures 8(a) and 8(b) show the corresponding diffraction patterns of the circular disks; Figs. 8(c) and 8(d) show one of the pollen-shaped objects. As can be seen from Figs. 8(a) and 8(b), there is a marked transition between randomly distributed disks and regularly oriented ones. Hence, the degree of randomness is important in interpreting the diffraction patterns. If distributed randomly, the total intensity is the sum of the intensities of each individual disk, which produces the well known ringlike structure. For the same number of disks arranged regularly on a quadratic array, the main characteristic is the interference pattern of the disks. This is easily explained by the array theorem, which states

that the diffraction pattern of an array of similar apertures is given by the product of the diffraction pattern from a single aperture and the diffraction (or interference) pattern of an identically distributed array of point sources.^{19,25} For the regularly distributed disks, the interference pattern of the square lattice is easily recognizable. In addition, one may still guess the ringlike structure of the single circular aperture, but it is not very prominent. For a structure with a degree of randomness in between these two extremes, one may readily observe ringlike structures that are superimposed by the interference structure owing to the more or less regular spacing. Although these changes of the diffraction patterns from random to regular arrangement of aperture arrays are well known, this new technique for generating samples of nearly arbitrary shape and distribution should prove useful for demonstration purposes. In the following, all results are presented for a purely random spatial distribution of the disks.

In contrast to the circular disks, the oriented



(a)



(b)

Fig. 10. Diffraction patterns of circular rings (simulating glories) for (a) white light and (b) laser light of $\lambda = 632.8$ nm.

pine-pollen-shaped scatterers with random spatial distribution [Figs. 8(c) and 8(d)] show distinct differences between random and preferential orientation of the disks. As was already observed for the white-light coronas (Fig. 6), random orientation of the disks leads to the usual circular coronas, whereas orientation results in diffraction patterns corresponding to the scatterer geometry. Figure 8(d) looks already similar to typical patterns of naturally observed elliptic coronas of the second kind¹³ (see Fig. 1) as well as to theoretical results using diffraction theory.¹⁴

Figure 9 shows the results for ellipsoids, which resemble the usual theoretical approximation to simulate birch pollen. Experimentally the axial ratio of the ellipsoids could easily be changed. In the analysis of earlier observations^{13,14} an aspect ratio in the range of 0.9 was assumed. Comparing the results of Fig. 9 with these observations [e.g., Fig.

1(a)] leads to good agreement for ratios of 0.85 to 0.9.

C. Other Possible Applications in the Field of Atmospheric Optics

The method can easily be extended to simulate the diffraction patterns of other atmospheric optical phenomena. For example, using ringlike structures or those with rings plus central spots are suitable for studying glories which, in the simple Fraunhofer diffraction approximation, can be regarded just as diffraction patterns formed by illuminated rings.^{26–28} As an example, Fig. 10 depicts the diffraction patterns of circular rings owing to white light and laser light. As is typical for glories, the angular size differs, and higher-order rings are more easily visible compared to circular disks.

4. Conclusions and Outlook

We report simple qualitative experiments that can be used to simulate the coronas caused by pollen. More quantitative laboratory experiments of this kind with monochromatic light sources allow comparison with theoretical modeling of such complex corona phenomena. The sample design program allows large changes of geometry, orientations, and randomness of spatial distributions. Therefore the diffraction patterns of arbitrarily shaped obstacles may be studied easily. The diffraction measurements are a quick way of testing which pollen shapes may give rise to newly observed natural coronas. Applications to other atmospheric optical phenomena such as, e.g., glories are possible.

References

1. J. M. Pernter and F. M. Exner, *Meteorologische Optik*, 2nd ed. (Braumüller, Wien, 1922).
2. M. G. J. Minnaert, *Light and Color in the Outdoors* (Springer-Verlag, Heidelberg, 1993).
3. R. A. R. Tricker, *Introduction to Meteorological Optics* (Elsevier, 1970).
4. R. Greenler, *Rainbows, Halos, and Glories* (Cambridge University, 1980).
5. D. K. Lynch and W. Livingston, *Color and Light in Nature* (Cambridge University, 1995).
6. L. Cowley, Ph. Laven, and M. Vollmer, "Rings around sun or moon: coronae and diffraction," *Phys. Educ.* **40**, 51–59 (2005).
7. H. C. van de Hulst, *Light Scattering by Small Particles* (Dover, 1981); reprint of 1957 edition.
8. C. F. Bohren and D. R. Huffman, *Absorption and Scattering of Light by Small Particles* (Wiley, 1983).
9. J. A. Lock and L. Yang, "Mie theory model of the corona," *Appl. Opt.* **30**, 3408–3414 (1991).
10. L. Cowley, IRIS Mie simulator, at <http://www.sundog.clara.co.uk/droplets/iris.htm>.
11. Ph. Laven, MiePlot simulator, at <http://www.philiplaven.com/mieplot.htm>.
12. J. A. Shaw and P. J. Neiman, "Coronas and iridescence in mountain wave clouds," *Appl. Opt.* **42**, 476–485 (2003).
13. P. Parviainen, C. F. Bohren, and V. Mäkelä, "Vertical elliptical coronas caused by pollen," *Appl. Opt.* **33**, 4548–4551 (1994).

14. E. Tränkle and B. Mielke, "Simulation and analysis of pollen coronas," *Appl. Opt.* **33**, 4552–4562 (1994).
15. R. C. Smith and J. S. Marsh, "Diffraction patterns of simple apertures," *J. Opt. Soc. Am.* **64**, 798–803 (1974).
16. Y. Takano and S. Asano, "Fraunhofer diffraction by ice crystals suspended in the atmosphere," *J. Meteorol. Soc. Jpn.* **61**, 289–300 (1983).
17. J. Scheiner and S. Hirayama, "Photographische Aufnahmen Fraunhofer'scher Beugungsfiguren," *Abh. Königl. Akad. Wiss. Berlin*, Appendix **1**, 1–13 (1894).
18. D. W. Schuerman, ed., *Light Scattering by Irregularly Shaped Particles* (Plenum, New York, 1980).
19. M. Born and E. Wolf, *Principles of Optics*, 7th ed. (Cambridge University, 1999); based on 1st edition from 1959.
20. F. A. Fischbach and J. S. Bond, "Fraunhofer diffraction patterns of microparticles," *Am. J. Phys.* **52**, 519–521 (1984).
21. F. A. Fischbach, "Interpretation of small angle light scattering maxima of single oriented microparticles," *Opt. Lett.* **10**, 523–525 (1985).
22. W. B. Schneider, H. Dittmann, program may be downloaded from <http://www.didaktik.physik.uni-erlangen.de/download/window.htm>.
23. G. Erdtman, *An Introduction to Pollen Analysis* (Chronica Botanica, Watham, Mass., 1954).
24. G. Erdtman, *Pollen and Spore Morphology/Plant Taxonomy: An Introduction to Palynology* (Almqvist&Wiksell, Stockholm, 1952, 1957), Vols. 1 and 2.
25. R. Guenther, *Modern Optics* (Wiley, 1990).
26. H. C. Bryant and A. J. Cox, "Mie theory and the glory," *J. Opt. Soc. Am.* **56**, 1529 (1966).
27. H. C. Bryant and N. Jarmie, "The glory," *Sci. Am.* **231**(7), 60–71 (1974).
28. M. J. Saunders, "Near-field backscattering measurements from a microscopic water droplet," *J. Opt. Soc. Am.* **60**, 1359 (1970).